Journal of Structural Geology 30 (2008) 1138–1149

Contents lists available at ScienceDirect

Journal of Structural Geology

journal homepage: www.elsevier.com/locate/jsg

Progressive deformation of a zone of magma transfer in a transpressional regime: The Variscan Mérens shear zone (Pyrenees, France)

Yoann Denèle, Philippe Olivier*, Gérard Gleizes

LMTG, Université de Toulouse, CNRS, IRD, OMP, 14 Avenue Edouard Belin, 31400 Toulouse, France

ARTICLE INFO

Article history:
Received 19 November 2007
Received in revised form 30 April 2008
Accepted 15 May 2008
Available online 28 May 2008

Keywords:
Mylonitic shear zone
Granite
AMS analysis
Transpression
Variscan
Mérens
Pyrenees

ABSTRACT

The EW-striking Variscan Mérens shear zone (MSZ), located on the southern border of the Aston dome (Pyrenees), corresponds to variously mylonitized gneisses and plutonic rocks that are studied using the Anisotropy of Magnetic Susceptibility (AMS) technique. The plutonic rocks form EW-striking bands with, from south to north, gabbro-diorites, quartz diorites and granodiorites. The MSZ underwent a mylonitic deformation with an intensity progressively increasing from the mafic to the more differentiated rocks. The foliations are EW to NW–SE striking and subvertical. A first set of lineations shows a moderate WNW plunge, with a dextral reverse kinematics. More recent subvertical lineations correspond to an uplift of the northern compartment. To the east, the MSZ was cut by a N120°E-striking late shear band, separating the MSZ from the Quérigut pluton. The different stages of mylonitization relate to Late Variscan dextral transpression. This regime allowed the ascent of magmas along tension gashes in the middle crust. We interpret the MSZ as a zone of magma transfer, which fed a pluton now eroded that was similar to the Quérigut and Millas plutons located to the east. We propose a model of emplacement of these plutons by successive pulses of magmas along en-échelon transfer zones similar to the MSZ.

1. Introduction

It is now generally accepted that the orogenic domains that underwent transpression were favourable sites to the ascent of magmas and to the emplacement of plutons because of the strong pressure gradients generated by such a regime (Hutton, 1997; Tikoff and Saint-Blanquat, 1997; Saint-Blanquat et al., 1998; Ferré et al., 2002; Koukouvelas et al., 2002; Romeo et al., 2006). In fact, only a small differential stress added to the lithostatic pressure allows a higher production of melt (Hand and Dirks, 1992) and/or a more efficient segregation and migration of this melt (Dell'Angelo and Tullis, 1988; Rutter and Neumann, 1995; Rushmer, 1996; Rabinowicz and Vigneresse, 2004). Major tectonic structures may play an important role by creating dilational space (D'Lemos et al., 1992; Tikoff and Teyssier, 1992; Román-Berdiel et al., 1997; Crawford et al., 1999). It has been proposed that sheet-like flow through crustal shear zone systems is the ascent mechanism of granitic magmas in convergent orogens (Brown and Solar, 1998a,b). However, though many studies dealing with magma transfer along shear zones have been published (Rosenberg et al., 1995; Druguet and Hutton, 1998; Benn et al., 1999; Brown and Solar, 1999), only few of them display a detailed petrographic and geometric description of the root zone and none gives quantitative data on the progressive deformation undergone by the granitic magmas emplaced in transpression.

The Variscan segment of the Pyrenees is a good example that documents the relationship that exists between deformation and emplacement of granitic plutons in transpressional contexts. Indeed, this segment is characterized by numerous calc-alkaline plutons emplaced in a dextral transpressive regime (Fig. 1a), as shown by systematic petrostructural studies (Leblanc et al., 1996; Gleizes et al., 1998, 2001, 2006; Auréjac et al., 2004; Román-Berdiel et al., 2004; Olivier et al., 2007). The main structural features observed in these plutons are sigmoidal magmatic lineation and foliation trajectories along with shear bands with dextral reverse movements (Fig. 1b). The country rocks display an EW-striking vertical foliation bearing horizontal lineations with a dextral component of shear (e.g. Evans et al., 1997). Moreover, this foliation "wraps" the plutons and forms asymmetrical neutral points, which agree with the dextral movement (Fig. 1b). The Variscan plutonism of the Pyrenees is dated between 312 and 305 Ma by the U/Pb zircon technique (Paquette et al., 1997; Roberts et al., 2000; Maurel et al., 2004; Olivier et al., 2004, 2007; Gleizes et al., 2006).

Various structural levels of plutons are exposed in the Variscan segment of the Pyrenees, yielding the rare opportunity to describe the shape of these plutons from the shallowest to the deepest parts. Their roofs are located in low grade metapelites ($T = 300$–400 °C,

* Corresponding author. Tel.: +33 5 61 33 25 95; fax: +33 5 61 33 25 60.
E-mail addresses: denele@lmtg.obs-mip.fr (Y. Denèle), olivier@lmtg.obs-mip.fr (P. Olivier).

0191-8141/$ – see front matter © 2008 Elsevier Ltd. All rights reserved.
doi:10.1016/j.jsg.2008.05.006

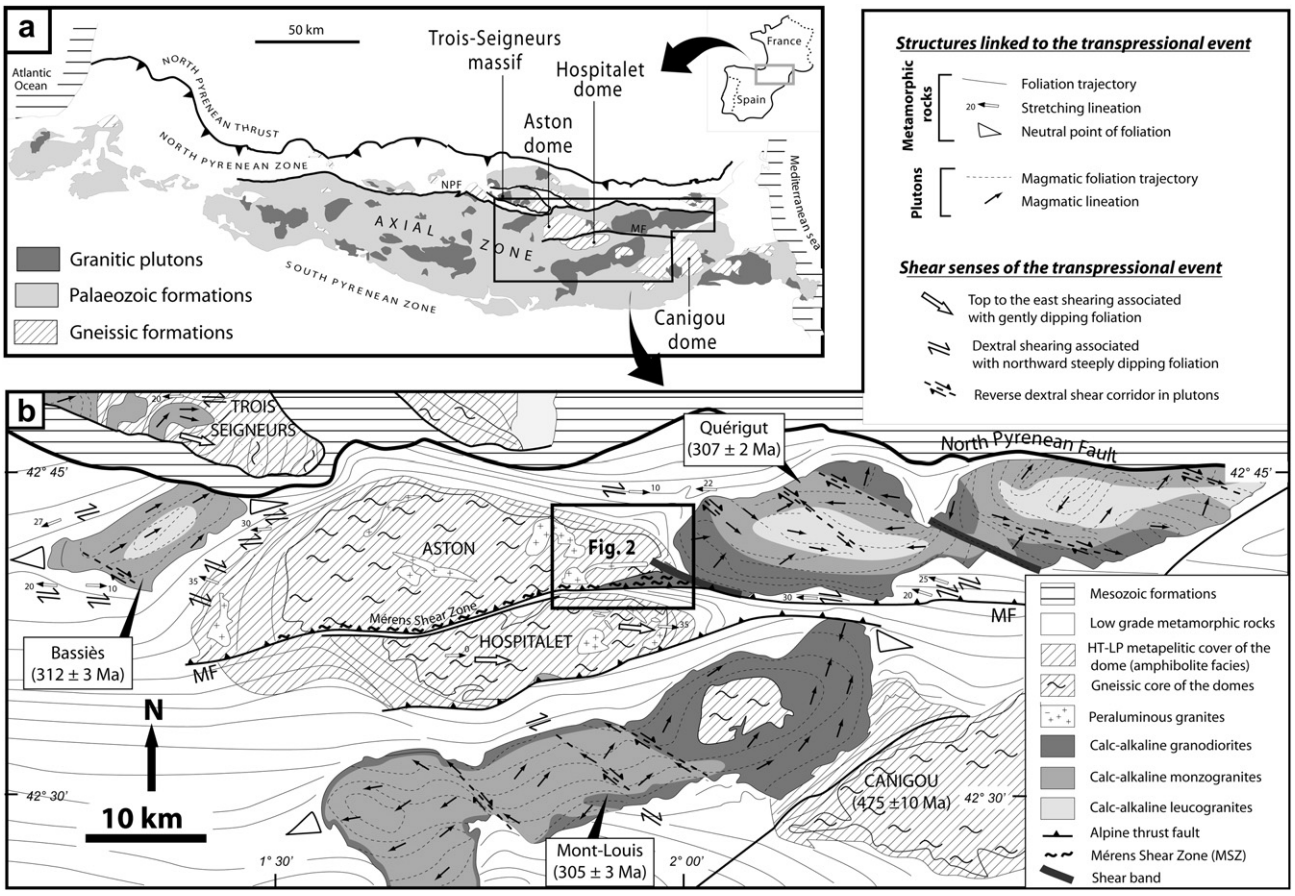

Fig. 1. Sketch maps of the Variscan segment of the Pyrenees. (a) The Variscan formations of the Pyrenees. NPF: North Pyrenean Fault. (b) Geological map of the Mérens shear zone (MSZ) and Mérens Fault (MF) area. The references for the structures and ages of the plutons are given in the text.

$P = 100$–200 MPa) and are dome-shaped, such as the Bassiès pluton (Gleizes et al., 1991) and the western part of the Mont-Louis pluton (Bouchez and Gleizes, 1995). The middle pluton levels, located in the biotite zone, are represented by downward bevelled and northward dipping, several kilometres wide, sheet-like intrusions such as the Quérigut pluton (Auréjac et al., 2004) and the central part of the Mont-Louis pluton. The lower pluton levels are located near the sillimanite isograd ($T > 600$ °C, $P = 300$–400 MPa) and are represented by steeply northward dipping, kilometre-thick sheets of magmatic rocks, such as the Trois-Seigneurs granite pluton (Leblanc et al., 1996).

In the Pyrenees, levels corresponding to the feeding zones of the plutons have not yet been described and the geometry and kinematics of these zones are unknown. Previous data suggest that these feeding zones could be located in the more or less migmatitic gneissic levels and could correspond to thin EW-striking subvertical bands of granitic to mafic rocks. In the central Pyrenees, such a band 10 km long is known and belongs to the Mérens shear zone (MSZ) which crosscuts the southern border of the Aston gneiss dome (Fig. 1b). In this paper, we present a petrostructural, microstructural and kinematic study realized in this elongate zone of granitic to mafic rocks and its gneissic country rocks. We show that the plutonic rocks belong to a zone of magma transfer for which we propose a model of formation and evolution.

2. Geological setting

The MSZ corresponds to an EW-striking, more than 70 km long, major Variscan shear zone separating the Aston gneiss dome to the north and the Hospitalet gneiss dome to the south (Fig. 1). This shear zone varies in thickness from some metres near its western extremity up to 2 km near the eastern extremity of the Aston Massif. Structural studies of the MSZ (Saillant, 1982; Mc Caig, 1984; Carreras and Cirés, 1986) have shown that reverse dextral movements took place along this band during Variscan times, the northern compartment being thrust onto the southern one. The MSZ is truncated to the south by the Alpine Mérens fault (MF), which brings into contact the MSZ and the country rocks of the Hospitalet orthogneisses (Carreras and Cirés, 1986; Barnolas and Chiron, 1996). In the studied area (Fig. 2), corresponding to the widest part of the MSZ, the rock formations affected by this shear zone are, from west to east, the orthogneisses and anatectic paragneisses of the Aston Massif, a band of calc-alkaline plutonic rocks and the southwestern border of the Quérigut pluton. The calc-alkaline rocks consist of mylonitic tonalites, gabbro-diorites, muscovite granites, pegmatites and aplites, and have been interpreted as forming an apophisis of the Quérigut pluton (Raguin, 1977). These plutonic rocks intrude the strongly anatectic paragneisses of the southern border of the Aston dome that are together mylonitized by the MSZ between ten to a hundred metres in width (Fig. 2).

The mineral paragenesis of the Aston paragneisses (biotite + sillimanite + garnet ± cordierite) yields P-T conditions around 300 MPa – 650 °C similar to those from other gneiss domes of the Pyrenees (Vielzeuf, 1996). This contrasts with the greenschist facies metapelites of the Hospitalet Massif that outcrop to the south of the MSZ, which implies a several kilometres vertical offset along this shear zone. To the north of the paragneisses, the Aston dome is made of orthogneisses similar to those of the Canigou Massif, which have been shown to derive from a thick laccolith of monzogranites

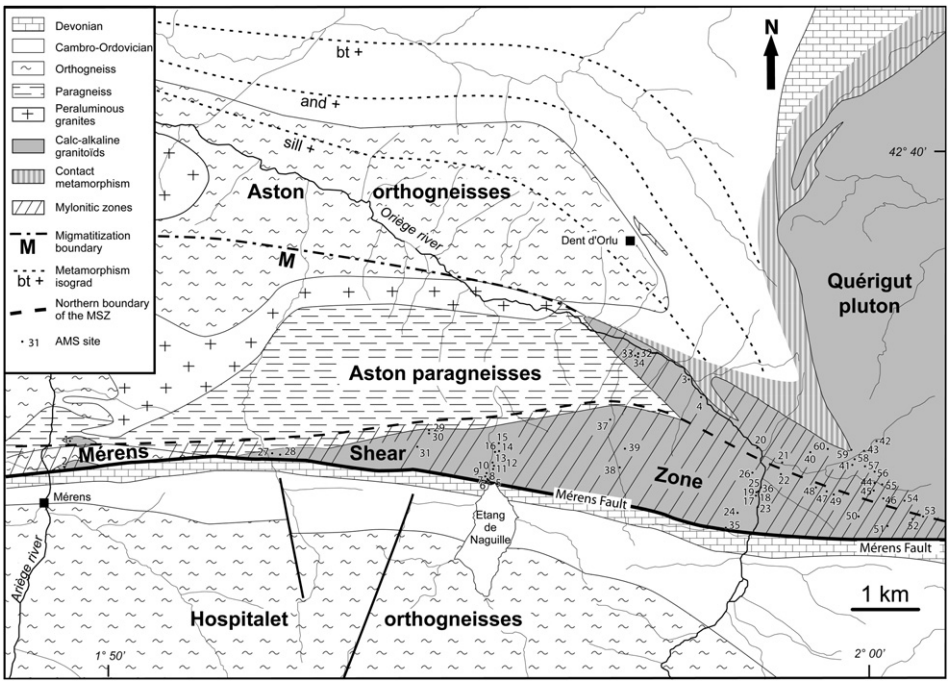

Fig. 2. Geological map of the studied area (after Raguin, 1977; Saillant, 1982; Besson, 1994; Barnolas and Chiron, 1996, modified) and location of the AMS sites.

dated at 475 ± 10 Ma (Deloule et al., 2002). Sills of peraluminous granites intrude both the paragneisses and the orthogneisses of the Aston dome. The largest one is located in-between the two types of gneisses. The cover of the orthogneisses to the north of the Aston dome consists of Upper Proterozoic to Lower Ordovician metapelites and Devonian marbles. This cover is characterized by a high temperature–low pressure (HT–LP) amphibolite-facies metamorphism, with a narrowing of the isograds near the core of the gneissic dome (Fig. 2). On the eastern part of this metamorphic cover, contact metamorphism related to the Quérigut pluton is superimposed. To the south of the Mérens Fault, the Hospitalet gneiss dome that formed during the Late Variscan dextral transpressive event D2 has been shown to correspond to a mega-fold overturned to the south (Denèle et al., 2007).

3. Structural study

3.1. The Aston dome

The part of the Aston dome located to the north of the plutonic rocks affected by the MSZ (Fig. 2) has a poorly known structure and kinematics. We therefore focussed our attention on the gneisses and their metapelitic cover of this part of the Aston dome in order to constrain the relationship between the plutonic rocks and their country rocks.

The gneisses and their micaschist cover show a strong pervasive deformation developed at high temperature. In the gneissic core and in the micaschists to the north, the foliations are mostly EW-striking, with a northward mean dip of 45° (Fig. 3a). To the east of the gneisses, the foliation of the micaschists progressively rotates to NS with 45° eastward dips. All these formations form the eastern periclinal extremity of the Aston dome. The cross-sections on Fig. 4a and b show the evolution of the foliation dips, which, from moderate in the anatectic paragneisses located near the MSZ, progressively steepen up to subvertical in the less metamorphic micaschist cover. In the metamorphic aureole of the Quérigut pluton, tight folds with a subvertical NS-striking cleavage are superimposed on the cleavage of the dome (Fig. 3a). The gneisses and micaschists display L–S fabrics. Two types of stretching lineations are observed (Fig. 3b): (i) NS to NE–SW trends with down-dip plunges, corresponding to a top to the south sense of shear; and (ii) EW to NW–SE trends with subhorizontal plunges, giving a top to the east sense of movement. The NS lineations are mainly observed in the northern part of the dome where the temperatures during deformation remained far from partial melting temperatures (~450 °C), whereas the EW lineations are mainly located in the southern part of the dome where deformation took place at temperatures close to migmatization (>650 °C).

3.2. The Mérens shear zone (MSZ)

Due to the extremely rugged topography, detailed field mapping of the MSZ, especially the part intruded by calc-alkaline granitic to mafic rocks, was not possible. Therefore, the data were mostly collected in a series of seven detailed NS-striking traverses. One of them cut across the gneisses that outcrop to the north of the Mérens village, while the other six transect the plutonic rocks (Figs. 2 and 3a).

Fabrics were measured either in the field or by using the AMS technique when the conditions of observation were not sufficiently good. The AMS technique applied to granitic rocks is detailed in several works to which the reader is invited to refer (Borradaile and Henry, 1997; Bouchez, 1997, 2000). This technique is based on the relationship that exists between magnetic and mineral fabrics in rocks. AMS measurements performed with a Kappabridge KLY-3 susceptometer allow the orientations and magnitudes of the three main axes $K1 \geq K2 \geq K3$ of the magnetic susceptibility ellipsoid to be determined. Their tensorial mean, measured on all the specimens of each site, defines the mean ellipsoid representative of the magnetic fabric of the site. From this mean ellipsoid, the average susceptibility ($Km = (K1 + K2 + K3)/3$), magnetic lineation (K1) and foliation (plane normal to K3), parallel to the mineral lineation and foliation, respectively, are determined. The granites of the Pyrenees being dominantly paramagnetic (Gleizes et al., 1993), Km is proportional to the iron content of the iron-bearing silicates. Therefore susceptibility can be directly correlated to the modal content in

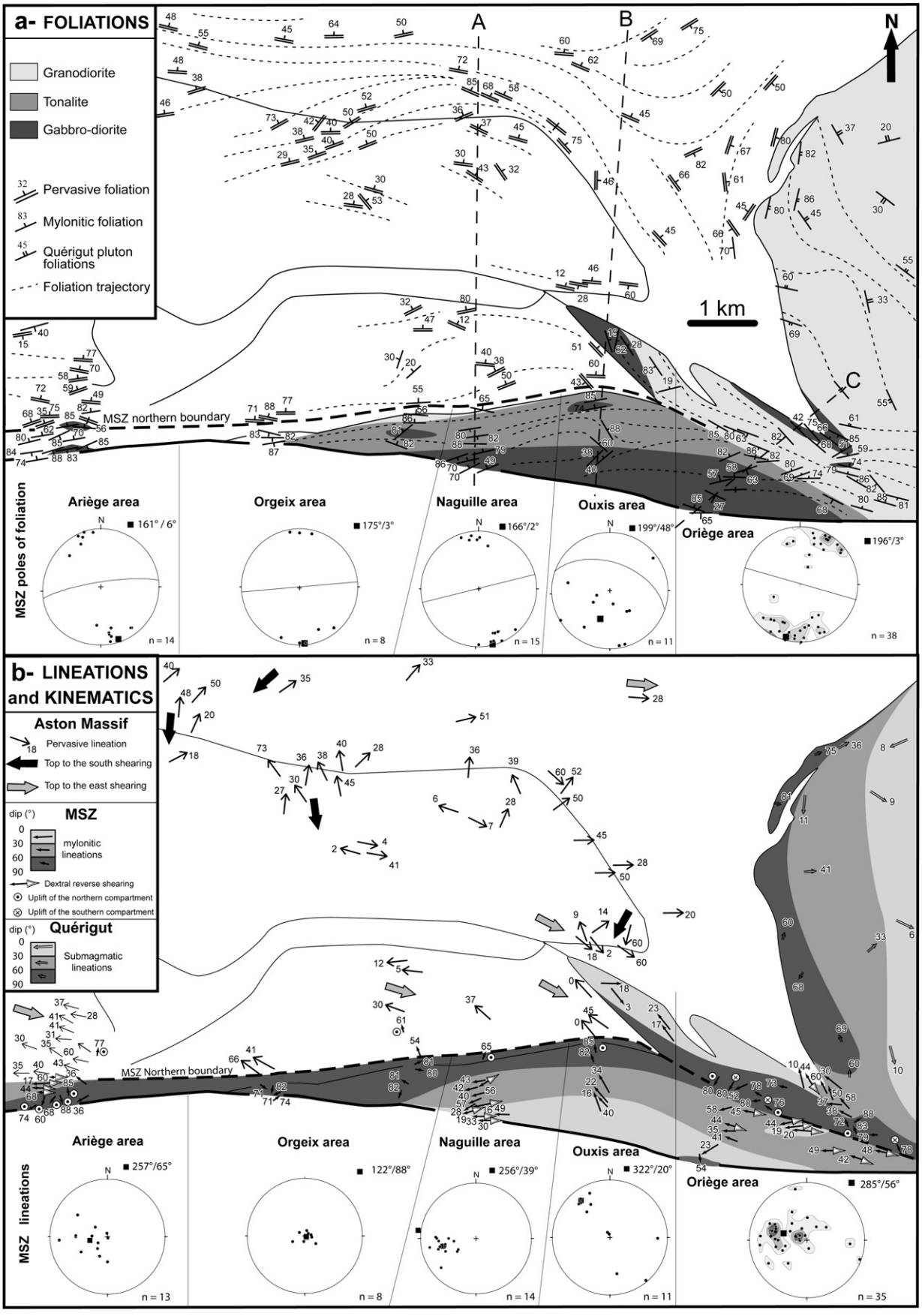

Fig. 3. Structural features of the eastern Aston Massif and of the plutonic rocks of the Mérens shear zone. (a) Foliations. A, B and C correspond to the location of the cross-sections of Fig. 9. (b) Lineations and associated kinematics. (Stereograms: Schmidt lower hemisphere; contours of the Oriège area: 2, 4, 6%). Structures in the Quérigut pluton are from Auréjac et al., 2004.

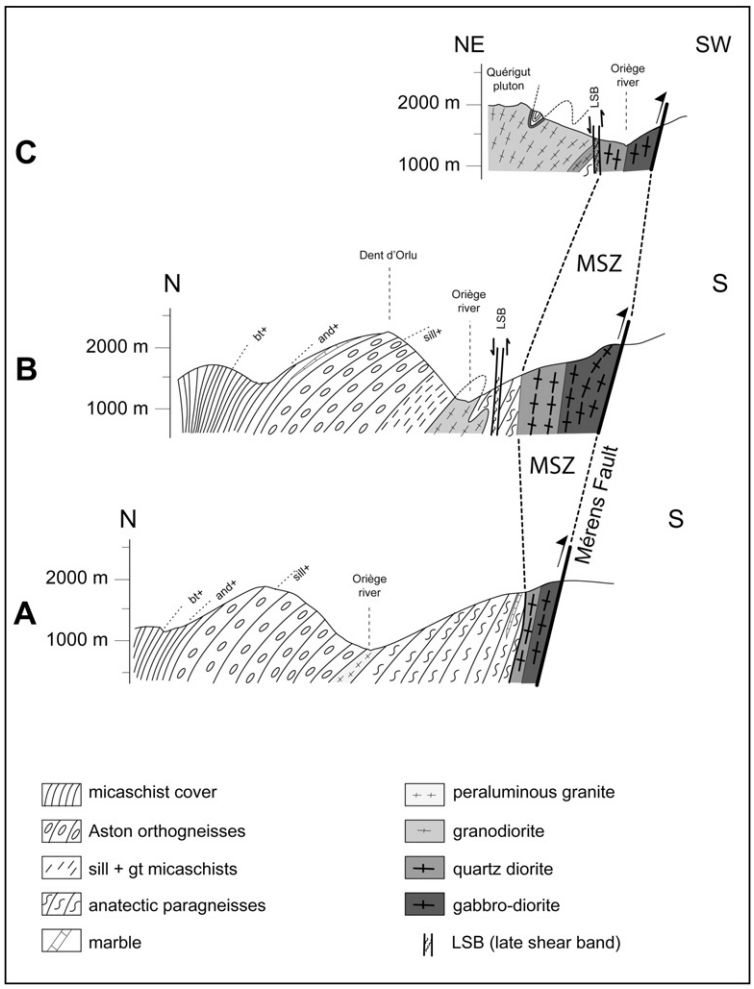

Fig. 4. Cross-sections of the studied area located on Fig. 3a.

biotite and amphibole principally. Moreover, in order to characterize the deformation within the MSZ, we have measured the magnetic anisotropy (Ppara% = 100[(K1 − *D*)/(K3 − *D*)−1]) where *D* is the diamagnetic contribution estimated at −14 μSI (Rochette, 1987), and the shape parameter ($T = \ln[K2^2/(K1 \times K3)]/\ln[K1/K3]$) of Jelinek (1981). In rocks dominated by paramagnetic carriers, several studies (e.g. Gleizes et al., 2001) have shown that the value of Ppara% correlates with the amount of deformation. The behaviour of the shape parameter *T* is more complex since it depends on both the deformation regime and the amount of biotite and amphibole in the specimen (Gleizes et al., 2006).

For the present study, specimens from plutonic rocks of the MSZ were collected from 61 sites (location on Fig. 2). The magnetic fabric measurements are given in Table 1, along with field structural measurements in order to compare these data sets.

3.2.1. Petrography and magnetic susceptibility of the plutonic rocks

Following optical microscopy examinations, five petrographic types were defined in the calc-alkaline granitic to mafic rocks of the MSZ which are, from the more differentiated ones to the mafic ones: (1) biotite + muscovite leucogranites; (2) biotite monzogranites; (3) biotite granodiorite; (4) biotite ± hornblende quartz diorite; and (5) biotite + hornblende gabbro-diorite. In addition to these magmatic parageneses, a secondary paragenesis linked to mylonitization is marked by biotite, epidote and muscovite. These rock types form roughly EW-striking bands consisting, from south to north, of gabbro-diorites, quartz diorites and granodiorites (Fig. 5). In the junction zone between the MSZ and the Quérigut pluton a N120°E-striking band appears essentially made of granodiorites containing a few stocks of gabbro-diorites. Finally, along the north-eastern border of the MSZ, close to the contact with the N120°E-striking band, lenses of monzogranite and leucogranite have also been observed.

The values of Km (μSI), ranging from 37 to 793, can be correlated with the previous rock types as follows (Fig. 5): leucogranite $25 < Km < 80$, monzogranite $135 < Km < 195$, granodiorite $204 < Km < 289$, quartz diorite $300 < Km < 397$, and gabbro-diorite $Km > 400$. Such a rather wide range of susceptibilities is commonly reported in the large plutons of the Pyrenees, as for instance the nearby Quérigut pluton (Auréjac et al., 2004), and reflects the diversity of the plutonic rocks of the MSZ.

3.2.2. Structures of the MSZ

The mylonitic foliation in the MSZ is EW-striking and steeply dipping (Figs. 4 and 6) with a mean at 87°N83° (strike and dip). The associated stretching lineation plunges to the west (mean at 274°/59°) with two groups of values, one being close to vertical and the other moderately plunging to the west (Fig. 6). There are, however, significant variations from one cross-section to the other (Fig. 3).

For the foliation (Fig. 3a), the stereonets of the western to central cross-sections (Ariège, Orgeix and Naguille areas) display very similar orientations with subvertical dips and mean strikes around N80°E. Such strikes are slightly oblique with respect to the orientation of the northern boundary of the MSZ. The stereonets of the

Table 1
AMS measurements of the plutonic rocks of the MSZ

Site	Rock types	Micro-structure	Km (μSI)	K1	Magnetic foliations	Field foliations	Field lineations	Pp%	*T*	Site	Rock types	Micro-structure	Km (μSI)	K1	Magnetic foliations	Field foliations	Field lineations	Pp%	*T*
1			498	306/36	96 N 56			2.9	0.64	31			400	302/81	50 N 81			5.0	0.2
2			747	240/46	66 S 85			4.2	−0.03	32			630	140/3	145 N 28	125 N 51		10.2	0.2
3			241	320/23	143 S 83	140 90		6.6	0.28	33			471	169/36	11 S 62	7 S 85		7.9	0.7
4			270	323/17	75 N 19			5.5	0	34			586	91/18	161 E 19			7.0	0.5
5	gbd	u	457	266/33	72 N 69	65 N 70		14.5	0.03	35			471	110/3	107 S 45	110 N 85		3.0	−0.05
6			537	270/49	66 N 70	60 N 75		8.8	−0.01	36	gbd	p	465	285/35	90 N 69	94 N 72		5.9	−0.23
7	gbd	p	490	230/19	48 N 84			5.3	−0.35	37			793	350/82	74 N 85	80 N 80		17.0	0.28
8	gbd	m	505	272/28	90 N 86			6.4	−0.24	38			423	158/16	45 N 40			10	0.6
9	gbd	p	511	263/57	74 N 83	80 N 75		14.8	−0.1	39			300	330/34	149 N 88			7.5	0.027
10	gbd	p	490	238/59	71 S 83			4.7	0.23	40	gnd	m	222	288/73	138 S 82	128 S 86	301/62	12.0	0.6
11	gbd	p	448	259/16	77 N 83			6.9	0.165	41	gnd	p	280	35/67	130 N 68			5.0	0.08
12	qd	m	397	247/40	66 N 88			8.1	0.56	42			257	1/58	102 N 61			8.0	−0.43
13	qd	m	307	257/34	88 S 74	95 N 85		11.3	0.68	43			657	295/30	117S 85			1.0	−0.9
14	lg	m	65	235/56	79 S 75	83 S 86		10.8	0.52	44	gbd	sub	415	296/38	103 N 74			3.0	0.69
15	qd	p	382	259/43	91 S 78	100 90		6.1	0.26	45	gnd	m	244	336/72	114 N 78	115 N 80		9.0	0.15
16	qd	m	306	255/42	82 S 82			9.8	0.401	46			276	338/83	122 N 86	120 N 86		7.4	−0.33
17	lg	m	25	290/42	84 N 64			3.4	−0.38	47	gnd	m	224	258/44	68 N 80			7.8	−0.46
18	gbd		468	293/41	70 N 51			9.5	−0.3	48	mg	m	172	264/19	67 N 69			8.3	−0.25
19	gbd	u	551	272/44	124 S 62			5.9	−0.82	49	mg	m	135	275/20	89 N 73			13.0	0.3
20	gnd	u	227	247/52	109 S 63	110 S 65		16.6	0.53	50	gnd	m	237	270/49	117 S 68			6.7	−0.14
21	lg	m	37	303/78	96 N 84	110 S 85		14.1	0.75	51	gnd	m	266	285/38	96 N 78	116 N 84	300/46	8.9	0.04
22	qd	m	393	285/43	105 90	92 N 84	277/48	9.5	0.15	52	gnd	m	271	269/48	89 N 90	117 N 87	299/48	9.1	−0.11
23	gbd	m	499	95/26	81 S 65	95 90		8.2	−0.5	53	mg	u	195	168/78	104 S 81	99 N 85	28/87	15.0	0.51
24	gbd	p	410	239/23	114 S 27	120 S 25		10.3	−0.16	54			289	277/79	140 S 83			8.0	0.25
25	gbd	p	651	219/47	72 S 63			6.7	−0.25	55			238				62/88	6.9	−0.38
26	qd	m	331	255/58	63 N 82			5.9	−0.18	56			247	318/58	78 N 62			9.3	0.79
27	lg	u	62	125/71	103 S 83	100 90		12.7	0.9	57	gbd	p	409	276/37	59 N 52			4.1	−0.02
28	lg	u	60	190/82	90 S 82	80 90		11.3	0.55	58	gbd	p	561		115 N 61	135 N 62	343/44	6.5	0.8
29	gnd	u	204	246/1	66 N 69			19.0	0	59	gbd	p	574	298/63	142 S 78	159 S 85		5.8	0.8
30			260	100/80	89 S 88	90 N 86		13.0	0.5	60			418	347/10	155 N 42	150 N 40		7.0	0.15

Rock types: gbd = gabbro-diorite, qd = quartz diorite, gnd = granodiorite, mg = monzogranite, lg = leucogranite. Microstructures: sub = subsolidus, p = protomylonite, m = mylonite, u = ultramylonite. Orientation of the linear structures corresponds to trend and plunge.

eastern cross-sections (Ouxis and Oriège areas) show a wider scattering, with a mean strike at N110°E and variable dips.

For the linear structures (Fig. 3b), the subvertical lineations are observed in all sectors except in the Naguille area, and the westward moderately plunging lineations are observed only in the Ariège, Naguille and Oriège sectors. Locally, in the Ouxis area, some lineations are NW–SE-trending and subhorizontal. In map view (Fig. 3b), all the lineation plunges increase from south to north, the lowest values (<30°) being located in the western part of the studied area near the Mérens Fault (Naguille, Ouxis and Oriège areas), whereas the highest plunges appear along the northern border of the MSZ.

The Oriège area which is at the junction between the EW and the N120°E-striking bands of plutonic rocks is especially interesting, so our sampling was distributed over a wider area. In the EW-striking mylonitic band, the foliation is mainly N80°E striking and subvertical. In the N120°E-striking band, the foliations are also subvertical but have a N120°E strike in the southeast and a N140°E strike in the northwestern part. Near the contact between the two bands, the strike of the foliation of the MSZ varies progressively from N80°E to N120°E. For the lineations, a clear difference also exists between the two bands: in the EW-striking band the lineations display a westward plunge of 40°, whereas they are subvertical in the N120°E-striking band.

3.2.3. Kinematics of the MSZ

Thirty-seven thin sections from the different rocks types were cut parallel to the XZ plane (perpendicular to foliation and parallel

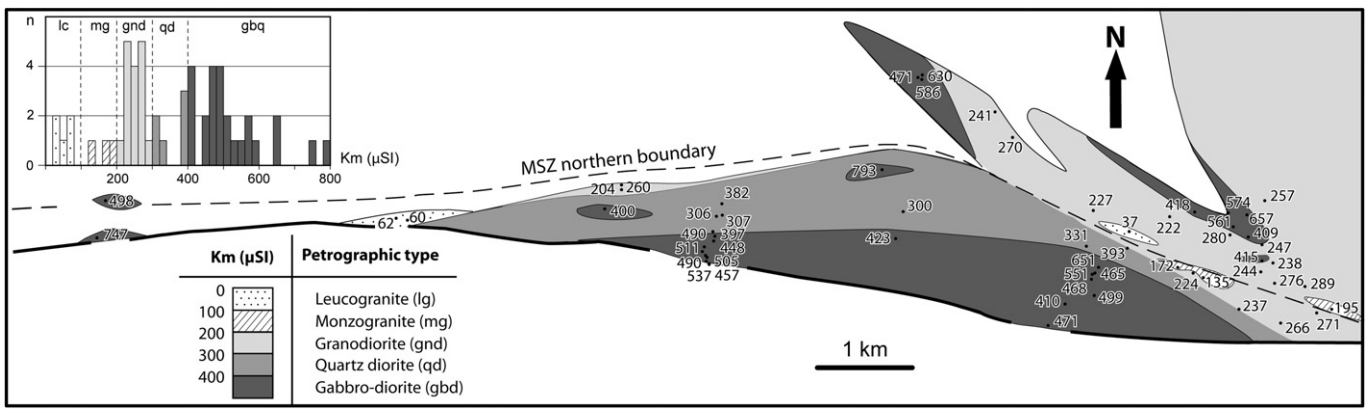

Fig. 5. Petrographic map and magnetic susceptibility values (Km) of the plutonic rocks of the studied area. The histogram shows the good correlation between petrographic types and Km values.

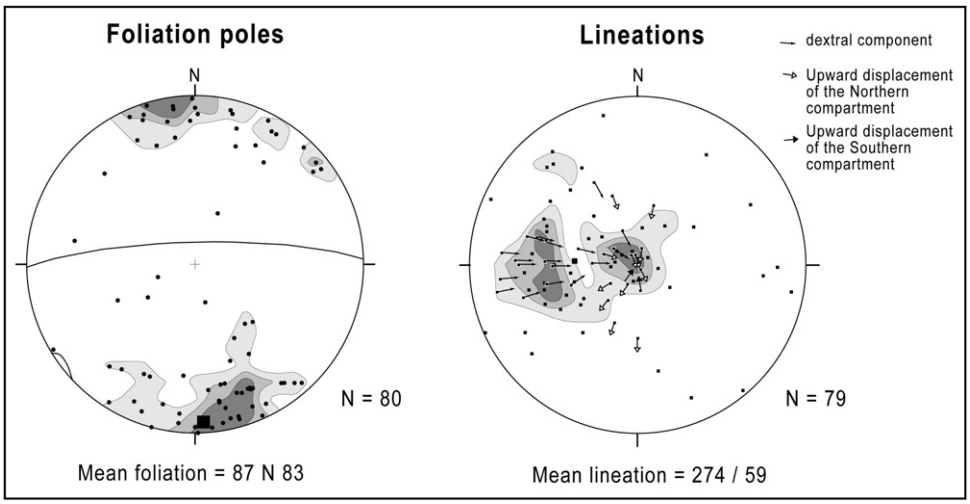

Fig. 6. Stereograms of the foliation poles and the lineations of all the AMS sites of the mylonitized plutonic rocks. (Schmidt lower hemisphere; contours: 1, 3, 5%). For the lineation diagram, the kinematics is indicated when available.

to lineation) in order to determine their sense of shear using the various criteria of noncoaxial deformation including mica fish, pressure shadows, δ-type mantled porphyroclasts, S/C structures, sigmoids of foliation trajectories and quartz *c*-axis fabrics. The sense of shear is different according to the different lineation sets. Eighteen amongst the 20 thin sections from the westward shallowly to moderately plunging lineations and within the steeply northward dipping foliations yield a well-defined reverse dextral sense of shear pointing to an uplift of the northern compartment (Figs. 3, 6, 7a and b). The senses of shear from the subvertical lineations are harder to determine. However, most of them call for an uplift of the northern compartment (12 thin sections amongst 17, Fig. 7c), except in the zone of junction between the two differently oriented plutonic rocks bands where they show an uplift of the southern compartment (3 thin sections amongst 17, Fig. 7d).

3.2.4. *Microstructure and magnetic anisotropy of the plutonic rocks of the MSZ*

A detailed microstructural analysis of the rocks of the MSZ was realized from 76 thin sections. Three main microstructural types were observed, namely protomylonitic, mylonitic and ultramylonitic depending on the percentage of recrystallized matrix (30, 30–80 and >80%, respectively). The protomylonitic microstructure (Fig. 7e) is mainly represented in the gabbro-diorites and is characterized by fractured plagioclase crystals infilled with biotite and quartz, by fractured amphiboles recrystallized on their periphery into biotite and epidote, and by recrystallized biotites. The matrix is mostly composed of small grains of quartz, biotite and epidote. The mylonitic microstructure is mainly present in the quartz diorites (Fig. 7f), which look like strongly foliated augen-gneisses, with subeuhedral and rather well preserved plagioclases in a matrix of small crystals of biotite, muscovite, quartz and epidote. The ultramylonitic microstructure is located along the northern border of the MSZ and, due to the very small grain size (<100 μm, Fig. 7c and d), the rock protolith is rather difficult to determine.

All these microstructures appear to result from a continuous deformation, from the solidus temperature to moderate temperatures in the solid state (600–500 °C) as attested by the presence of plagioclases undergoing bending (i.e. deformed at a temperature higher than their plasticity threshold), then fracturation and finally being included in a recrystallized matrix. In the Pyrenees, these rather high temperatures in rocks undergoing a continuous deformation characterize the Variscan event (Barnolas and Chiron, 1996). By contrast, the Alpine deformation, observed up to 10 m from the contact of the Mérens fault, is characterized by mylonites with chloritized biotites and calcite in late fractures.

The magnetic anisotropy Pp% varies between 1 and 19 (Table 1 and Fig. 8a) with a mean at 8.2. These values show a good correlation with the microstructural types (Fig. 8a). The microstructures are protomylonitic when $5 < Pp\% < 8$, mylonitic when $8 < Pp\% < 11$, and ultramylonitic when $Pp\% > 10\%$. The few samples with $Pp\% < 5$ correspond to slightly deformed rocks essentially located near or within the Quérigut pluton. In map view, the microstructural types and the corresponding values of Pp% form various zones of isodeformation. The most striking feature is the presence of a strongly deformed corridor located along the northern border of the MSZ characterized by ultramylonites and $Pp\% > 11$. This corridor also corresponds to the most silicic rock types, namely granodiorites, monzogranites and leucogranites (Fig. 5). The anisotropy decreases to the south of this corridor, the microstructures becoming mylonitic in the granodiorites and in the northern part of the quartz diorites, then protomylonitic in the gabbro-diorites and in the southern border of the quartz diorites. To the northwest of this corridor, the anisotropy decreases abruptly southwards with $5 < Pp\% < 8$ corresponding mainly to protomylonitic microstructures. However, some areas are less deformed ($Pp\% < 5$) when approaching the border of the Quérigut pluton. It may be noted that a site of gabbro-diorite (site 43, Fig. 2), belonging to this pluton, has a very low degree of anisotropy (1%) corresponding to a weak subsolidus deformation.

3.2.5. *Type of fabric and shape parameter* T *of the plutonic rocks of the MSZ*

The shape parameter T (Jelinek, 1981) characterizes the shape of the AMS ellipsoid and hence the type of magnetic fabric. For $T < 0$, the fabric is linear (or prolate), for $0 < T < 0.3$ it is plano-linear, for $0.3 < T < 0.5$ it is planar (or oblate) and for $T > 0.5$ it is strongly planar. In the MSZ, the values of T vary strongly between −0.9 and 0.9. As for Pp%, the distribution in map view of the parameter T (Fig. 8b) shows a clear zonation. Globally, the fabric is planar ($S > L$) to strongly planar ($S \gg L$) in the strongly anisotropic corridor located along the northern border of the MSZ. The linear fabric appears to the southeast in the gabbro-diorites and granodiorites. To the northeast of the MSZ, the fabrics are plano-linear ($S \sim L$) in the N120°E-striking band of plutonic rocks and linear ($L > S$) in the western boundary of the Quérigut pluton.

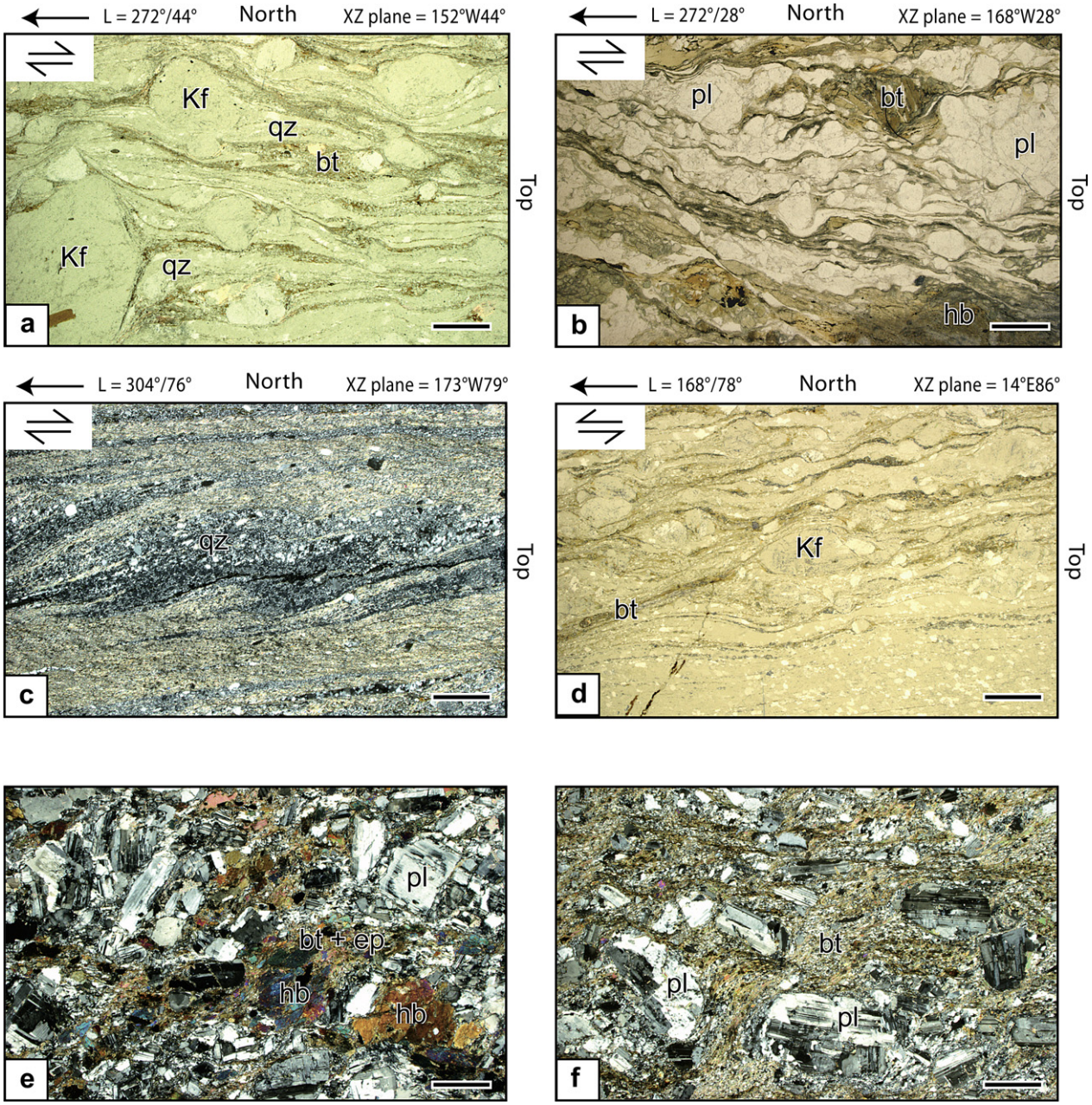

Fig. 7. Microphotographs of various rock types and deformations of the MSZ. Part figures (a)–(d) are XZ sections and (e) and (f) are non oriented sections. (a) Aston mylonitic orthogneiss close to the Mérens village. (b) Mylonitic hb-bearing gabbro-diorite of the Naguille area (site 9). (c) Ultramylonitic leucogranite in the Oriège area (site 21). (d) Ultramylonitic orthogneiss in the Oriège area (site 53). (e) Protomylonitic gabbro-diorite of the Naguille area (site 11). (f) Mylonitic quartz diorite of the Naguille area (site 16). Photographs (a), (b) and (d): plane polarized light, (c), (e) and (f): crossed polars. Scale-bar: 1 mm; bt = biotite, ep = epidote, hb = hornblende, Kf = K-feldspar, mu = muscovite, pl = plagioclase, qz = quartz.

4. Discussion

4.1. Intensity of the mylonitic deformation in the MSZ in relation with the petrographic types

A good correlation is observed in the MSZ between the magnetic anisotropy values and the different microstructural types (Fig. 8a), as is also seen in other plutonic rocks from the Pyrenees, for example the Quérigut pluton (Auréjac et al., 2004). Fig. 7 demonstrates the relative independence between the AMS parameters and the petrographic types. For a given facies, as for instance the gabbro-diorites, there are very variable values of Pp% [3;11] and T [−0.9;0.9]. However, the detailed analysis of the Naguille cross-section (Fig. 9) displays a correlation between Km and Pp% on the one hand and Km and T on the other hand. Indeed, the quartz diorites, which are characterized by the lowest Km values, show high Pp% values [8;12], planar fabrics ($0.26 < T < 0.7$) with mylonitic microstructures, whereas the gabbro-diorites, which are characterized by higher Km values, show lower Pp% values [5;7], linear fabrics ($-0.6 < T < 0.2$) with protomylonitic microstructures, except close to the Mérens Fault where Pp% reach 15 because of the Alpine deformation.

The quartz diorites and the gabbro-diorites being deformed during the same event (Fig. 3), the observed differences in Pp% and T values between the two rocks types can be explained by the different mineralogical compositions at the origin of contrasted

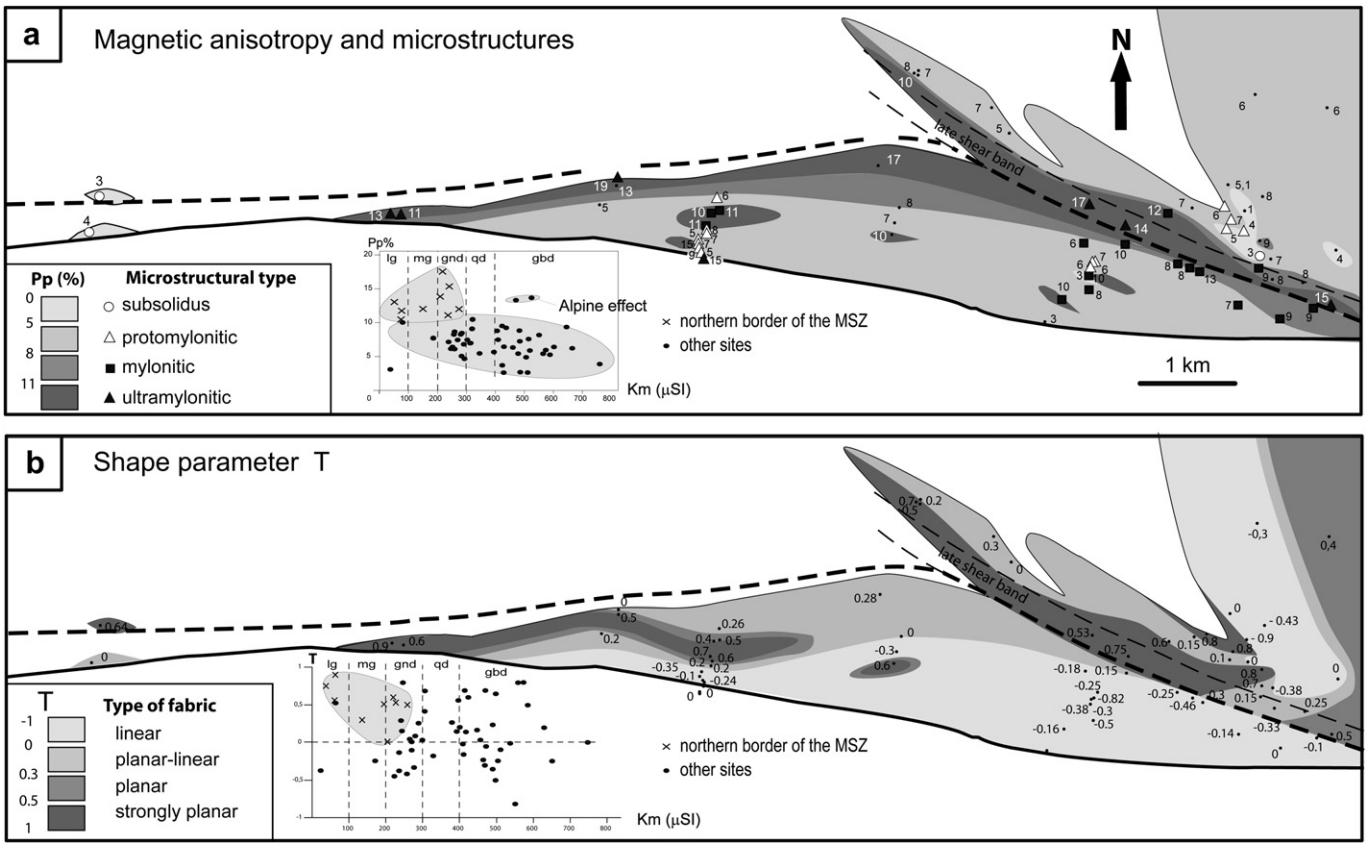

Fig. 8. Characterization of the deformation in the mylonitized plutonic rocks. (a) Anisotropy of the magnetic susceptibility correlated with the microstructural types. (b) Shape parameter *T*.

rheological behaviours. The quartz diorites, containing a large amount of quartz and mica, have a plasticity threshold lower than the temperature of deformation of the MSZ. Therefore, they underwent an important plastic deformation with a strong planar fabric controlled by the biotite flakes. In contrast, the gabbro-diorites, essentially composed of plagioclase and hornblende, are much less plastic at the temperature of deformation of the MSZ. Consequently, their deformation is mostly protomylonitic and their more linear fabrics agree with a dominant control by hornblende. In other words, within the P-T conditions of the MSZ, the quartz diorites were more incompetent than the gabbro-diorites which acted as a more rigid core.

This rheological control by petrography may be applied to the whole MSZ, the intensity of the mylonitic deformation progressively increasing from the mafic to the more silicic rocks. The highest deformation is localized in the latest granitic injections to the north of the MSZ and along the N120°E-striking late shear band which deflects the structures of the MSZ and displays ultramylonitic microstructures.

4.2. The MSZ: a dextral reverse ductile fault corresponding to a zone of magma transfer

Some authors have proposed that the root zones of plutons emplaced in a transpressive regime correspond to areas where magma feeders are concentrated (Rosenberg et al., 1995; Benn et al., 1999; Brown and Solar, 1999). The root zones are generally sheet-like, associated with shear zones and elongated parallel to the regional structures. Thus the band of plutonic rocks of the MSZ made of sheets of gabbro-diorite, quartz diorite and granodiorite, parallel to the Variscan segment of the Pyrenees, and located at deep level, may be considered as a root zone. Petrographically, this band shows a calc-alkaline suite comparable to that of the Quérigut pluton (Raguin, 1977), demonstrating that all the calc-alkaline magmas were transferred through this root zone, and also that the magmatic differentiation took place below the level of observation.

This root zone displays strong HT solid state deformation, with high magnetic anisotropies (5–17%) typical of the deepest parts of the Pyrenean plutons (e.g. Leblanc et al., 1996). All these characteristics underline the link that exists between a transfer zone of magma and the formation of a shear zone in a transpressive context. The mylonitic foliations and lineations observed in this shear zone correspond to two different stages: first a reverse dextral movement into the MSZ compatible with the emplacement of a pluton and then, subvertical displacements along the northern border of the MSZ and in the N120°E-striking late shear band that we interpret as a shortening ending the magma transfer stage.

4.3. Model of emplacement of the plutons of the eastern Pyrenees

We have seen that two sets of lineations have been observed in the Aston dome, one N–NE-trending with a top to the south sense of shear and the other EW-trending with a top to the east sense of shear. We interpret the first set, which is exclusively located in the northern border of the orthogneisses and in the metapelitic country rocks, as the result of an early deformation because these lineations have a trend and a sense of shear similar to those of the Canigou orthogneisses (Soliva et al., 1989) which have been attributed to an early Variscan event of crustal thickening. We attribute this event to the early middle pressure gradient defined by Mezger et al. (2004).

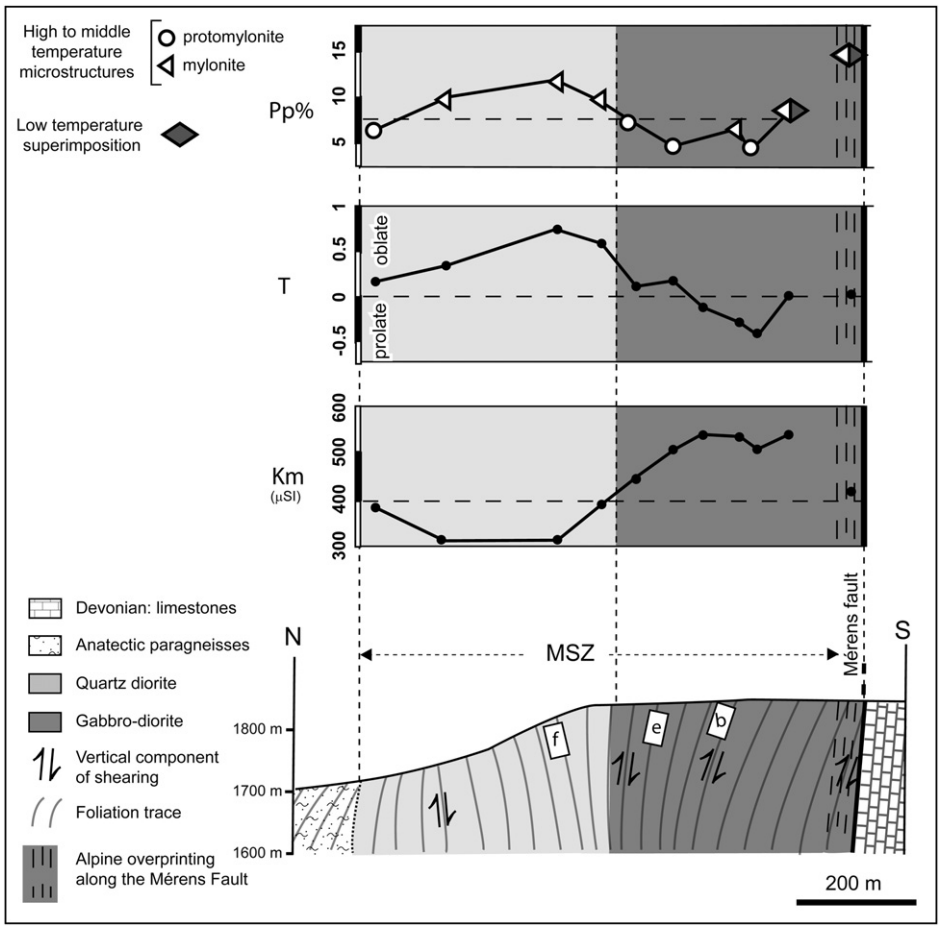

Fig. 9. Cross-section of the Naguille area (below) and corresponding AMS scalar parameters Km, *T* and Pp% with microstructures. Fig. 6(b), (e) and (f) correspond to the microphotographs on Fig. 7.

By comparison with a recent study in the nearby Hospitalet dome (Denèle et al., 2007), the second set of lineations is interpreted as a transposed structure observed in the migmatitic zone of the Aston dome and formed during an eastward lateral flow in the middle crust submitted to a transpressive regime. Subsequently, all the structures were progressively tilted to the north during the same regime. This tilting may correspond to the formation of the northern limb of an EW-trending mega-fold in the Aston Massif, comparable to the mega-fold described in the Hospitalet dome.

Given that the plutonic rocks of the MSZ cut across the Aston dome structures (Figs. 3 and 4), magmas injection through the MSZ must have taken place after the tilting. The same chronology between magmatism and transpression has been described in the Hospitalet dome from the study of calc-alkaline granitic stocks (Fig. 1) which are injected in the southern border of the orthogneisses (Denèle et al., 2007).

The ascent of magmas was achieved through successive injections since several petrographically homogeneous parallel bands, with sharp contacts, constitute the MSZ. A similar interpretation has been deduced from structural and geochemical studies in the Quérigut calc-alkaline pluton (Roberts et al., 2000; Auréjac et al., 2004).

The geological map (Fig. 1b) shows, from west to east, the succession of the plutonic rocks of the MSZ, of the Quérigut pluton and of the Millas pluton. These three granitic units share several petrographic and structural similarities, among which a NS zonation with mafic rocks to the south and more silicic rocks to the north. Auréjac et al. (2004) showed that the Quérigut pluton was formed during a dextral transpressive regime and that its root zone was an EW-trending sheet of mafic rocks steeply dipping to the north.

To explain magma emplacement in a transpressive regime, it is necessary to create dilational spaces. Among the different models that have been proposed to account for the formation of such openings (e.g. D'Lemos et al., 1992; Tikoff and Teyssier, 1992; Román-Berdiel et al., 1997), those which are compatible with a regular spacing between plutons are either tensional bridges (Tikoff and Teyssier, 1992) or tensional gashes (Hutton, 1988).

In the case of the Eastern Pyrenees where the plutons are regularly spaced, the model of tensional bridge is not applicable because the NE-SW-striking internal structures of the Quérigut and Millas plutons do not fit with this model, which implies that these structures would be NW-SE striking. Therefore the tension gash model (Fig. 10a), formed as a consequence of the dextral transpressive regime, is favoured. At the beginning, these gashes were infilled with successive batches of gabbro-dioritic, quartz dioritic and granodioritic magmas (Fig. 10a). Following this, the Mérens, Quérigut and Millas plutons grew, along with the emplacement of central monzogranitic and leucogranitic magmas (Fig. 10b). During the same event, in the upper levels of the plutons N120°E-trending shear bands characterized by HT reverse dextral movements took place and, in the root zone mylonitization developed, characterized by westward plunging lineations. Subsequently, ultramylonitization with vertical motions developed at the northern border of the MSZ. Finally, by the end of the crystallization of the most evolved magmas, the Mérens shear zone and the two N120°E-trending late shear bands (see Fig. 1b) with vertical

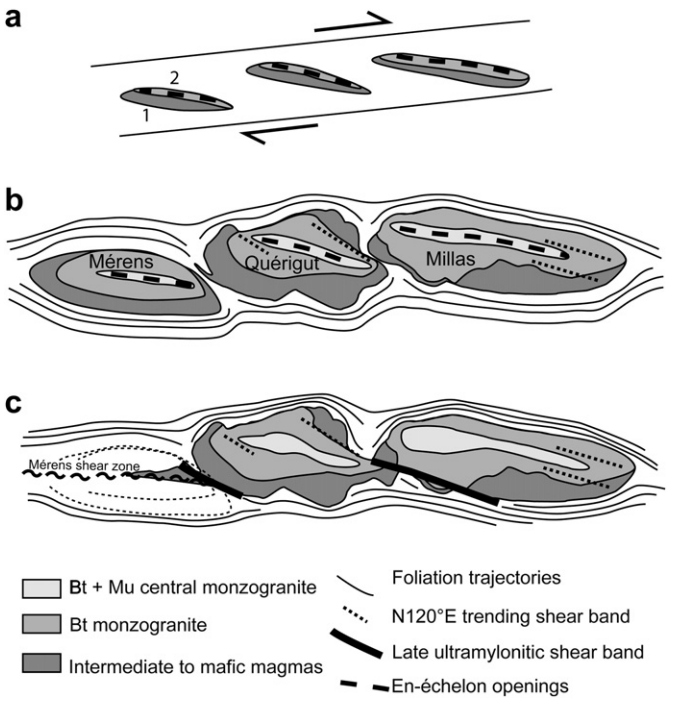

Fig. 10. Schematic model of formation and evolution of three plutons (Mérens, Quérigut, Millas) of the eastern Pyrenees in dextral transpressive regime. (a) Infilling of the tension gashes by successive magmas batches, (1) mafic to intermediate magmas, successively gabbro-diorite, quartz diorite and granodiorite and (2) monzogranitic magmas; (b) growth of the plutons; (c) formation of the two N120°E-striking late shear band in-between the plutons.

movements developed, the first one separating the MSZ from the Quérigut pluton, and the second one separating the Quérigut pluton from the Millas pluton (Fig. 10c). These shear bands resulted from the localization of the deformation that took place between the contiguous plutons which became rigid. At the present time, the upper levels of the Mérens pluton, which was probably situated above the roof of the Aston orthogneisses, have been eroded because of the important exhumation of the Aston Massif.

5. Conclusion

The band of plutonic rocks of the MSZ shows the features of a magmas transfer zone which fed a large pluton, presently removed by erosion. The transpressive regime has favoured the creation of gashes in the middle crust and the ascent of magmas from the zone of production in the basal parts of the crust up to their sites of emplacement in the upper crustal metapelitic cover. This study demonstrates also that the magmatic differentiation took place in the lower crust.

This band has been submitted to a progressive Variscan deformation which resulted in various types of mylonites and protomylonites in the earlier emplaced mafic rocks up to ultramylonites in the later emplaced silicic rocks. The mylonitization is compatible with a Late Variscan dextral transpressive regime.

The model proposed in this paper strengthens the relationship existing between transpression and magma ascent. Initially, dilational spaces were created in the middle crust along reverse strike-slip faults. Several successive pulses of magma flowed through these conduits. Finally, the magmas lubricated the fault zones and were responsible for the increasing localization of deformation and for the development of shear zones as wide as the root zones.

Acknowledgements

We thank P. Barbey and J.L. Bouchez for constructive discussions, M. Jessell for proof-reading the manuscript, J.B. Auréjac for his participation in the sampling of the Mérens shear zone along the Lake of Naguille cross-section, C. Cavaré-Hester for drawings, F. de Parseval and J.-F. Mena for thin sections making. We also thank J. Mezger and an anonymous reviewer for their very useful remarks.

References

Auréjac, J.-B., Gleizes, G., Diot, H., Bouchez, J.L., 2004. Le complexe granitique de Quérigut (Pyrénées, France) ré-examiné par la technique de l'ASM: un pluton syntectonique de la transpression dextre hercynienne. Bulletin de la Société géologique de France 175, 157–174.

Barnolas, A., Chiron, J.C., 1996. Synthèse géologique et géophysique des Pyrénées. Introduction. Géophysique. Cycle hercynien. BRGM/ITGE, Orléans/Madrid.

Benn, K., Roest, W.R., Rochette, P., Evans, N.G., Pignotta, G.S., 1999. Geophysical and structural signatures of syntectonic batholith construction: the South Mountain Batholith, Meguma Terrane, Nova Scotia. Geophysical Journal International 136, 144–158.

Besson, M., 1994. Neuf coupes à travers le massif de l'Aston. Géologie de la France 4, 21–33.

Borradaile, G.J., Henry, B., 1997. Tectonic applications of magnetic susceptibility and its anisotropy. Earth-Science Reviews 42, 49–93.

Bouchez, J.L., 1997. Granite is never isotropic: an introduction to AMS studies of granitic rocks. In: Bouchez, J.-L., Hutton, D.H.W., Stephens, W.E. (Eds.), Granite: From Segregation of Melt to Emplacement Fabrics. Kluwer Academic Publishers, Dordrecht, pp. 95–112.

Bouchez, J.L., 2000. Anisotropie de susceptibilité magnétique et fabrique des granites. Comptes Rendus de l'Académie des Sciences, Paris 330, 1–14.

Bouchez, J.L., Gleizes, G., 1995. Two-stage deformation of the Mont-Louis Andorra granite pluton (Variscan Pyrenees) inferred from magnetic susceptibility anisotropy. Journal of the Geological Society, London 152, 669–679.

Brown, M., Solar, G.S., 1998a. Shear zone systems and melts: feedback relations and self-organization in orogenic belts. Journal of Structural Geology 20, 211–227.

Brown, M., Solar, G.S., 1998b. Granite ascent and emplacement during contractional deformation in convergent orogens. Journal of Structural Geology 20, 1365–1393.

Brown, M., Solar, G.S., 1999. The mechanism of ascent and emplacement of granite magma during transpression: a syntectonic granite paradigm. Tectonophysics 312, 1–33.

Carreras, J., Cirés, J., 1986. The geological significance of the western termination of the Mérens fault at Port Vell (Central Pyrenees). Tectonophysics 129, 99–114.

Crawford, M.L., Klepeis, K.A., Gehrels, G., Isachsen, C., 1999. Batholith emplacement at mid-crustal levels and its exhumation within an obliquely convergent margin. Tectonophysics 312, 57–78.

Dell'Angelo, L.N., Tullis, J., 1988. Experimental deformation of partially melted granitic aggregates. Journal of Metamorphic Geology 6, 495–516.

Deloule, E., Alexandrov, P., Cheilletz, A., Laumonier, B., Barbey, P., 2002. In-situ U–Pb zircon ages for Early Ordovician magmatism in the eastern Pyrenees, France: the Canigou orthogneisses. International Journal of Earth Sciences (Geologische Rundschau) 91, 398–405.

Denèle, Y., Olivier, Ph., Gleizes, G., Barbey, P., 2007. The Hospitalet gneiss dome (Pyrenees) revisited: lateral flow during Variscan transpression in the middle crust. Terra Nova 19, 445–453.

D'Lemos, R.S., Brown, M., Strachan, R.A., 1992. Granite magma generation, ascent and emplacement within a transpressional orogen. Journal of the Geological Society, London 149, 487–490.

Druguet, E., Hutton, D.H.W., 1998. Syntectonic anatexis and magmatism in a mid-crustal transpressional shear zone: an example from the Hercynian rocks of the eastern Pyrenees. Journal of Structural Geology 20, 905–916.

Evans, N.G., Gleizes, G., Leblanc, D., Bouchez, J.-L., 1997. Hercynian tectonics in the Pyrenees: a new view based on structural observations around the Bassiès granite pluton. Journal of Structural Geology 19, 195–208.

Ferré, E., Gleizes, G., Caby, R., 2002. Obliquely convergent tectonics and granite emplacement in the Trans-Saharan belt of Eastern Nigeria: a synthesis. Precambrian Research 114, 199–219.

Gleizes, G., Leblanc, D., Bouchez, J.-L., 1991. Le pluton granitique de Bassiès (Pyrénées ariégeoises): zonation, structure et mise en place. Comptes Rendus de l'Académie des Sciences, Paris 312, 755–762.

Gleizes, G., Nédélec, A., Bouchez, J.L., Autran, A., Rochette, P., 1993. Magnetic susceptibility of the Mont-Louis Andorra ilmenite-type granite (Pyrenees): a new tool for the petrographic characterization and regional mapping of zoned granite plutons. Journal of Geophysical Research 98, 4317–4331.

Gleizes, G., Leblanc, D., Santana, V., Olivier, Ph., Bouchez, J.-L., 1998. Sigmoidal structures featuring dextral shear during emplacement of the Hercynian granite complex of Cauterets–Panticosa (Pyrenees). Journal of Structural Geology 20, 1229–1245.

Gleizes, G., Leblanc, D., Olivier, Ph., Bouchez, J.-L., 2001. Strain partitioning in a pluton during emplacement in transpressional regime: the example of the Néouvielle granite (Pyrenees). International Journal of Earth Sciences (Geologische Rundschau) 90, 325–340.

Gleizes, G., Crevon, G., Asrat, A., Barbey, P., 2006. Structure, age and mode of emplacement of the Hercynian Bordères-Louron pluton (Central Pyrenees, France). International Journal of Earth Sciences (Geologische Rundschau) 95, 1039–1052.

Hand, M., Dirks, P.H.G.M., 1992. The influence of deformation on the formation of axial-planar leucosomes and the segregation of small melt bodies within the migmatitic Napperby Gneiss, central Australia. Journal of Structural Geology 14, 591–604.

Hutton, 1988. Granite emplacement mechanisms and tectonic controls: inferences from deformation studies. Transactions of the Royal Society of Edinburg: Earth Sciences 79, 245–255.

Hutton, D.H.W., 1997. Syntectonic granites and the principle of effective stress: a general solution to the space problem? In: Bouchez, J.-L., Stephens, W.E., Hutton, D.W.H. (Eds.), Granite: From Melt Segregation to Emplacement fabrics. Kluwer Academic Publishers, pp. 189–197.

Jelinek, V., 1981. Characterization of the magnetic fabric of rocks. Tectonophysics 79, 563–567.

Koukouvelas, I., Pe-Pipper, G., Piper, D.J.W., 2002. The role of dextral transpressional faulting in the evolution of an early Carboniferous mafic–felsic plutonic and volcanic complex: Cobequid Highlands, Nova Scotia, Canada. Tectonophysics 348, 219–246.

Leblanc, D., Gleizes, G., Roux, L., Bouchez, J.-L., 1996. Variscan dextral transpression in the French Pyrenees: new data from the Pic des Trois-Seigneurs granodiorite and its country rocks. Tectonophysics 261, 331–345.

Maurel, O., Respaut, J.-P., Monié, P., Arnaud, N., Brunel, M., 2004. U–Pb emplacement and $^{40}Ar/^{39}Ar$ cooling ages of the eastern Mont-Louis granite massif (Eastern Pyrenees, France). Comptes Rendus Geoscience 336, 1091–1098.

Mc Caig, A.M., 1984. Fluid-rock interaction in some shear zones from the Pyrenees. Journal of Metamorphic Geology 2, 129–141.

Mezger, J.E., Passchier, C.W., Régnier, J.-L., 2004. Metastable staurolite–cordierite assemblage of the Bossòst dome: Late Variscan decompression and polyphase metamorphism in the axial zone of the central Pyrenees. Comptes Rendus Géoscience 336, 827–837.

Olivier, Ph., Gleizes, G., Paquette, J.-L., 2004. Gneiss domes and granite emplacement in an obliquely convergent regime: new interpretation of the Variscan Agly Massif (Eastern Pyrenees, France). In: Whitney, D.L., Teyssier, C., Siddoway, C.S. (Eds.), Gneiss Domes in Orogeny. Geological Society of America, Special Paper, vol. 380, pp. 229–242.

Olivier, Ph., Gleizes, G., Paquette, J.-L., Muñoz Sáez, C., 2007. Structure and U–Pb dating of the Saint-Arnac pluton and the Ansignan charnockite (Agly Massif): a cross-section from the upper to the middle crust of the Variscan Eastern Pyrenees. Journal of the Geological Society, London 164, 1–12.

Paquette, J.-L., Gleizes, G., Leblanc, D., Bouchez, J.-L., 1997. Le granite de Bassiès (Pyrénées): un pluton syntectonique d'âge westphalien. Géochronologie U–Pb sur zircons. Comptes Rendus de l'Académie des Sciences, Paris 324, 387–392.

Rabinowicz, M., Vigneresse, J.L., 2004. Melt segregation under compaction and shear channelling: application to granitic magma segregation in a continental crust. Journal of Geophysical Research B109, doi:10.1029/2002JB002372.

Raguin, E., 1977. Le massif de l'Aston dans les Pyrénées de l'Ariège. Bulletin du BRGM 2, 89–119.

Roberts, M.P., Pin, C., Clemens, J.D., Paquette, J.L., 2000. Petrogenesis of mafic to felsic plutonic rock associations: the calc-alkaline Quérigut complex, French Pyrenees. Journal of Petrology 41, 809–844.

Rochette, P., 1987. Magnetic susceptibility of the rock matrix related to magnetic fabric studies. Journal of Structural Geology 9, 1015–1020.

Román-Berdiel, T., Gapais, D., Brun, J.P., 1997. Granite intrusion along strike-slip zones in experiment and nature. American Journal of Science 297, 651–678.

Román-Berdiel, T., Casas, A.M., Oliva-Urcia, B., Pueyo, E.L., Rillo, C., 2004. The main Variscan deformation event in the Pyrenees: new data from the structural study of the Bielsa granite. Journal of Structural Geology 26, 659–677.

Romeo, I., Capote, R., Tejero, R., Lunar, R., Quesada, C., 2006. Magma emplacement in transpression: the Santa Olalla Igneous Complex (Ossa-Morena Zone, SW Iberia). Journal of Structural Geology 28, 1821–1834.

Rosenberg, C.L., Berger, A., Schmid, S.M., 1995. Observations from the floor of a granitoid pluton: inferences on the driving force of final emplacement. Geology 23, 443–446.

Rushmer, T., 1996. Melt segregation in the lower crust: how have experiments helped us? Transactions of the Royal Society of Edinburgh: Earth Sciences 97, 73–83.

Rutter, E.H., Neumann, D.H.K., 1995. Experimental deformation of partially molten Westerly granite under fluid-absent conditions with implications for the extraction of granitic magmas. Journal of Geophysical Research 100 (B8), 15697–15716.

Saillant, J.P., 1982. La faille de Mérens (Pyrénées-Orientales) microstructures et mylonites. 3^{e} cycle thesis, Paris 7 Univ., 291 pp.

Saint-Blanquat, M.de, Tikoff, B., Teyssier, C., Vigneresse, J.L., 1998. Transpressional kinematics and magmatic arcs. In: Holdsworth, R.E., Strachan, R.A., Dewey, J.F. (Eds.), Continental Transpressional and Transtensional Tectonics. Geological Society, London, Special Publications, vol. 135, pp. 327–340.

Soliva, J., Salel, J.F., Brunel, M., 1989. Shear deformation and emplacement of the gneissic Canigou thrust nappe (Eastern Pyrenees). Geologie en Mijnbouw 68, 357–366.

Tikoff, B., Saint-Blanquat, M.de, 1997. Transpressional shearing and strike-slip partitioning in the Late Cretaceous Sierra Nevada magmatic arc, California. Tectonics 16, 442–459.

Tikoff, B., Teyssier, C., 1992. Crustal-scale, en echelon "P-shear" tensional bridges: a possible solution to the batholithic room problem. Geology 20, 927–930.

Vielzeuf, D., 1996. Les massifs nord-pyrénéens à soubassement granulitique. In: Barnolas, A., Chiron, J.C. (Eds.), Synthèse géologique et géophysique des Pyrénées. Introduction. Géophysique. Cycle hercynien, vol. 1. BRGM/ITGE, pp. 502–521.